

Self-organized structures in $\text{CoCr}_2\text{O}_4(001)$ thin films: Tunable growth from pyramidal clusters to a $\{111\}$ fully faceted surface

U. Lüders, F. Sánchez, and J. Fontcuberta

Institut de Ciència de Materials de Barcelona, CSIC, Campus U.A.B., Bellaterra 08193, Catalunya, Spain

(Received 14 October 2003; revised manuscript received 11 February 2004; published 6 July 2004)

Self-organized pyramidal structures (quadratic or hut-cluster type) of ferrimagnetic spinel CoCr_2O_4 (CCO) are grown by deposition from vapor phase on $\text{MgAl}_2\text{O}_4(001)$ substrates. The surfaces of the structures, forming an angle $\Theta \approx 50\text{--}55^\circ$ with the (001) surface, are identified as the spinel $\{111\}$ facets, so the pyramids can be considered as true three-dimensional objects. Important characteristics of the structures can be tuned by varying the deposition time and/or growth temperature. It allows one to obtain isolated $\{111\}$ pyramids self-ordered in arrays along $\langle 110 \rangle$ directions or fully $\{111\}$ faceted surfaces. The size and size distribution of the objects can be controlled by varying the fabrication conditions: the observed bimodal distribution obtained at low temperatures transforms into a single-modal one in films grown at high temperature. Moreover, the equilibrium shape of CCO islands is pyramidal for any object size, which is key for the controlled fabrication of nano-objects. The driving forces for the observed $\{111\}$ faceted objects and surfaces, bimodal size distributions and long range order are discussed. We end by discussing the (dis)similarities of the growth of the spinel CCO structures with that of the widely studied of silicon-germanium semiconductor dots and underlining prospects for new functionalities of self-ordered growth of complex oxides.

DOI: 10.1103/PhysRevB.70.045403

PACS number(s): 81.07.-b, 68.65.-k

INTRODUCTION

Self-organized growth of nanometric objects on surfaces has attracted much attention in the last decade due to its interest in nanoscience promising new technological applications. Such potential is well recognized in the field of semiconductors, and the self-organized growth of these materials is being studied intensely.¹⁻³ The usefulness of nanostructures relies on the ability to obtain narrow size distributions of islands of similar shape. Indeed, well-defined distributions have been found in some semiconducting systems, although quite commonly multimodal size distributions with differently shaped islands are observed. The growth of $\text{Si}_x\text{Ge}_{1-x}$ (SiGe) alloys on Si(001) by a Stranski-Krastanow mechanism has received particular attention.¹⁻⁹ The three-dimensional (3D) growth gives rise to pyramids and hut clusters with base dimensions of a few tens of nanometers and having $\{105\}$ facets. These facets are at only an angle of 11.3° from the surface plane, and therefore the corresponding aspect ratio is rather low. The formation of these structures is understood as due to the partial relief of the elastic energy of the coherently strained film material.¹⁻⁹ It is also well known that above a critical size there is a shape transition to multifaceted domes.¹⁻⁹ The domes have a lower chemical potential due to the more efficient elastic energy relief of these structures, and therefore their faster growth results in bimodal size distributions.¹⁻⁹

In spite of the renewed interest in oxides in science and technology, self-ordered growth of oxides has yet to be explored much. In this paper we shall report on the growth of 3D islands of CoCr_2O_4 (CCO). CCO is a ferrimagnetic insulating oxide with a spinel structure, with a Curie temperature of about 100 K that has recently received some attention for its use as a template for the growth of epitaxial thin films of ferrites as well as a barrier in magnetic tunnel junctions.^{10,11}

We will show that under appropriate conditions, the growth of CCO on $\text{MgAl}_2\text{O}_4(001)$ presents a self-ordered pattern of pyramids and hut clusters having $\{111\}$ facets. It will be demonstrated that the object number and size distribution characteristics can be tuned by varying the growth time and/or the growth temperature. The driving forces for the observed shape, size distributions, and long-range order will also be discussed.

EXPERIMENT

CCO films were deposited on single crystalline MgAl_2O_4 (MAO) substrates by rf magnetron sputtering. MAO and CCO are isostructural, although there is an important lattice mismatch ($\sim 3\%$) between both materials. All the films were prepared at the same pressure of 0.25 Torr (25% O_2 –75% Ar), and different substrate temperatures in the 600–800°C range, and with deposition times between 10 and 400 min. X-ray diffraction characterization¹² indicated that the films are epitaxial, with a $[100]\text{CoCr}_2\text{O}_4(001)/[100]\text{MgAl}_2\text{O}_4(001)$ epitaxial relationship, and fully relaxed. A sample corresponding to 15-min deposition time was smooth and thick enough to present interference peaks in x-ray reflectometry measurement. From the data of reflected intensity,¹³ a growth rate of about 1.7 nm/min was deduced. We note, however, the difficulty to define a thickness accurately because of the important roughness associated with the pyramidal growth to be described below. Therefore, when comparing films, it is more reliable to use the deposition time as a label for the thickness. Magnetic measurements¹² showed that the films are ferrimagnetic with a Curie temperature of ≈ 100 K, in good agreement with the corresponding measurement performed on the polycrystalline sputtering target. The film morphology was inves-

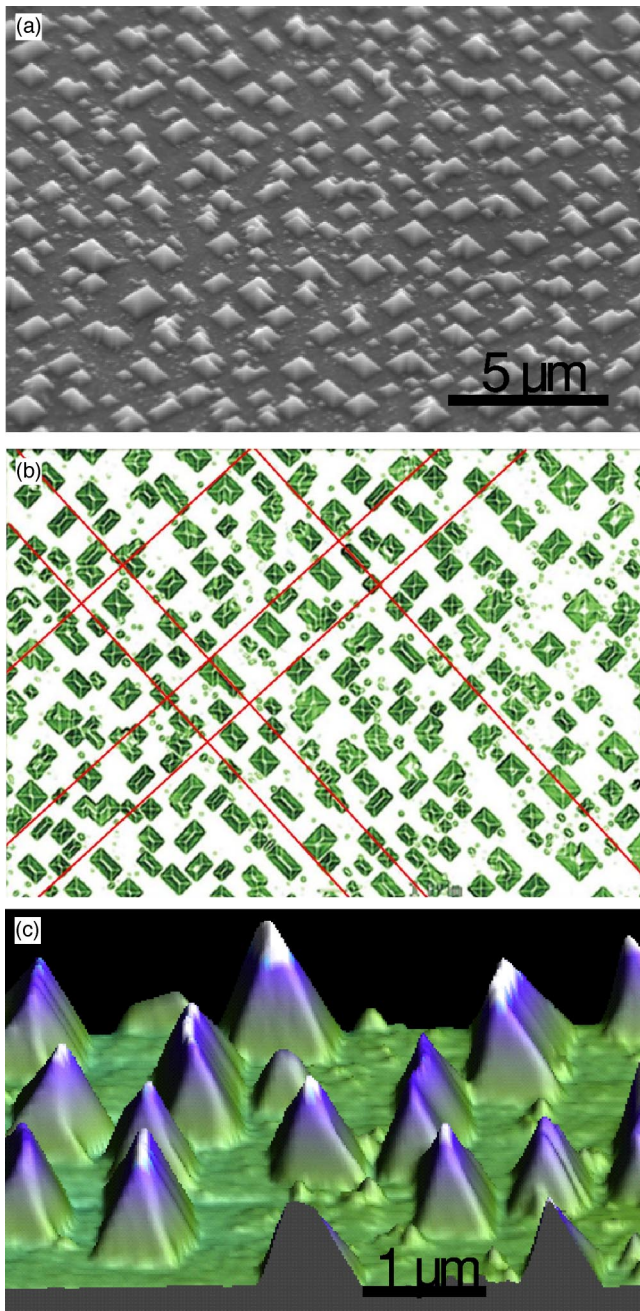


FIG. 1. (Color online) Morphology of a film deposited at 600°C during 200 min: (a) SEM 45° view; (b) SEM 0° view after applying a derivative filter. A few lines along the $[110]$ and $[1-10]$ directions are drawn guides to the eye to illustrate that there is a preferential positioning of pyramids along some $\langle 110 \rangle$ directions; (c) AFM 3D view.

tigated by scanning electron microscopy (SEM) and by atomic force microscopy (AFM) working in tapping mode.

RESULTS

We first show a SEM image [Fig. 1(a)] of the surface of a film deposited during 200 min at 600°C . The most obvious, striking, feature is the presence of islands with dimensions

up to about 1 micrometer and having a very well-defined shape with square or rectangular base, i.e., pyramids or huts. The well-defined shape strongly suggests the island surfaces to be crystalline facets. In addition to having such particular individual shape, the islands show a collective order: they are perfectly oriented along the $\langle 110 \rangle$ crystal directions, and they are usually around $1\ \mu\text{m}$ apart. Moreover, as indicated by the solid lines in Fig. 1(b), the objects appear to be preferentially positioned along certain well-defined $[110]$ and $[1-10]$ directions. Closer inspection of the SEM image also shows the presence of a collection of smaller islands (100–200 nm) having the same shape as the large ones. More precise information on the island morphology and height values was obtained from AFM scans. Figure 1(c) shows an AFM image (3D view) corresponding to the same sample. The height of the square-based pyramids and hut clusters is up to 400 nm. Even more noticeable than such large values is that the lateral surfaces of the islands form an angle $\Theta \approx 50\text{--}55^{\circ}$ with the substrate plane. The dispersion in the measured angles is due to the convolution of the film topography and the AFM tip. Also, the finite size of the AFM tip explains that some islands have a shape that is not perfectly symmetric. Within the experimental error of the AFM measurement, the lateral surfaces are likely to be $\{111\}$ facets, which form an angle $\Theta = 54.7^{\circ}$ with the (001) plane. It has to be remarked that the large Θ value implies that the aspect ratio of the islands is very high and thus they are true 3D objects. The observation of 3D objects with a micrometric size and well-defined shape and facets is definitely unusual in thin film deposition processes. The AFM image also emphasizes the existence of smaller islands, 10–100 nm high and 70–200-nm base dimension, as already observed in the SEM pictures.

In order to explore the morphology evolution with the deposition conditions, four samples were prepared at the same substrate temperature (600°C) and with 50, 100, 200, and 400 min of sputtering time. In Fig. 2 the corresponding SEM images (45° views and derivatives of 0° views) are shown. It can be noted that the film of lower nominal thickness (50 min) presents [Fig. 2(a)—left] a structure similar to that described in Fig. 1 (600°C and 200 min), although the size of the islands is smaller. The biggest islands at 50 min have dimensions above 200 nm. In spite of the small size, their faceted morphology and pyramidal shape (quadratic or hut type) is clearly resolved in the derivative image [Fig. 2(a)—right]. Moreover, in Figs. 2(a) a collection of smaller—nanometric— islands, having dimensions around 100 nm, are also visible. We note that all objects are $\{111\}$ faceted irrespectively of size.

Comparing the evolution of the film's morphology [Figs. 2(a)–2(d)], we observe that the size of the larger islands increases with the deposition time, while a family of islands with dimensions around 200 nm is found in all the samples. These trends were confirmed by a quantitative analysis of the evolution of the dimensions of the objects. It was performed by measuring the length and width (long and short axis of the island base, respectively) of around 150 islands from each sample and fitting Gaussian functions to the histograms. In Fig. 3, panel (a) shows the histogram of the 400-min sample

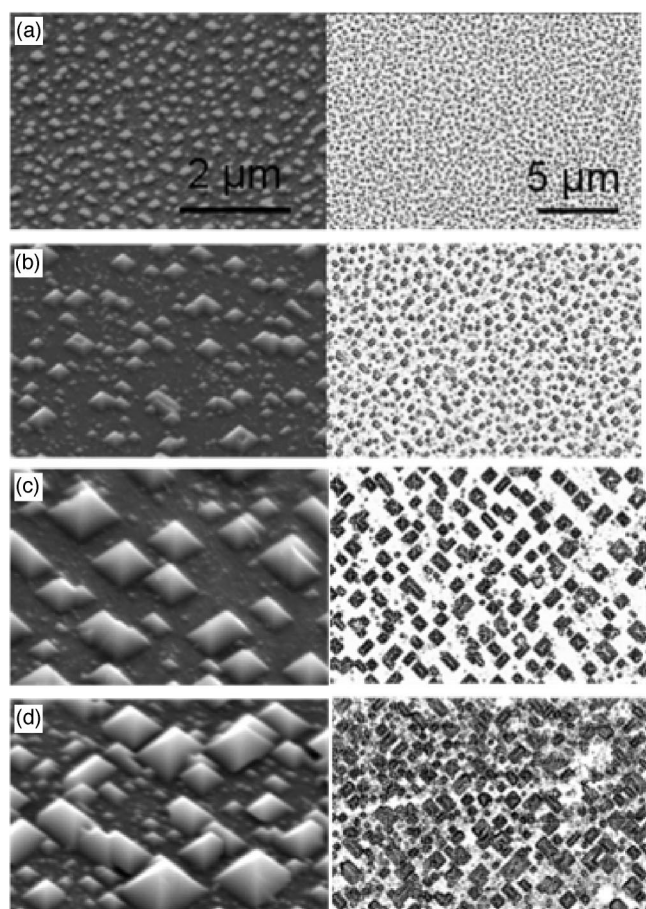


FIG. 2. Scanning electron microscopy images (45° view) of films deposited at 600°C during (a) 50 min; (b) 100 min; (c) 200 min; and (d) 400 min. At the right of each image are lower magnification images, 0° view and after applying a derivative filter, of the same images.

and the two fitted Gaussian functions. In panel (d) the maxima of the distributions are indicated by points, whereas the bars correspond to the full width at half maximum of the Gaussian functions corresponding to each family. This plot clearly shows that the bimodal size distribution develops progressively, i.e., the difference of the size of the two island families increases with deposition time (whereas for the thinner films the maxima of length distribution are at about 200 and 100 nm, they grow up to 1000 and 300 nm, respectively, for the thicker ones). Note also that increasing the sputtering time causes the distributions to become notably broader.

We turn now to the dependence of the film morphology on the growth temperature. Figure 4 shows SEM images of films prepared during the same sputtering time (200 min) but at different substrate temperatures from 600 to 750°C . Visual inspection of these images immediately reveals that, in the explored temperature range, the size of the islands is reduced progressively as the deposition temperature increases. Even more, when the deposition temperature rises, not only is the size of the objects reduced to around 200 nm, but also the size distribution becomes notably narrower and the bimodal distribution is no longer observable. In Fig. 3 the histograms of length and of width [panels (b) and (c), respec-

tively], corresponding to the sample prepared at 750°C are plotted. The quantitative analysis [see Fig. 3(e)] of these images has been performed as indicated above. The influence of the temperature is evidenced by the comparison between these histograms and that of the sample grown at 600°C [panel (a)]. Interestingly, it can be also appreciated in Fig. 4 that the degree of coverage of the film surface with CCO pyramids becomes higher when raising the deposition temperature. In fact, as evidenced by the 45° SEM view in the inset of Fig. 4(c), corresponding to the sample prepared at 700°C , most of the islands are in contact, and so they form a $\{111\}$ fully faceted surface. The same morphology is evidenced in the sample prepared at 750°C .

We have also prepared films at high temperature (750°C) during longer and shorter sputtering times to investigate the formation and evolution of the $\{111\}$ fully faceted surface. In an earlier stage (100-min sputtering time) the surface is not yet fully faceted, but there is a well-ordered structure of small islands that have similar sizes [Fig. 5(a)]. Note that although the coverage is nearly 100%, most of the islands remain isolated. With additional incorporation of material this surface becomes $\{111\}$ fully faceted, as was observed in the sample prepared during 200-min sputtering time [Fig. 4(d)]. Interestingly, after a very long growth time of 400 min the morphology is very similar: the surface remains $\{111\}$ fully faceted [Fig. 5(b)]. This implies that the $\{111\}$ fully faceted CCO surface constitutes a highly stable system. Such stability makes this structured surface easy and reproducible to fabricate, contrary to self-organized semiconductor surfaces.

DISCUSSION

We have observed that the CCO objects maintain their well-defined pyramidal shape during growth, having sizes ranging from a few tens of nanometers up to above 1 micron. This finding contrasts with the behavior found in other systems, such as SiGe ,¹⁻⁹ where a shape transition to multifaceted domes takes place at much smaller island sizes. It has to be noted that the surface energy in spinels is strongly anisotropic,¹⁴ with the $\{111\}$ planes having the minimal energy. In fact, the calculations of Mishra and Thomas¹⁴ indicate that the surface energy of the $\{111\}$ planes is around 5 times lower than that of $\{100\}$ surfaces, and close to 10 times lower than that of the $\{110\}$ planes. Such extreme difference explains the shape of the CCO crystallites, since the total energy, which depends on the total area and the surface energy, can be minimized with the formation of the low surface-energy structures. According to the Wulff construction, the equilibrium shape of a crystal with such extreme anisotropy is a $\{111\}$ faceted octahedron. In agreement with the theoretical predictions,¹⁵ the spinel octahedral shape is commonly seen in single crystals. The CCO crystallites reported here are not free, as they have grown on a substrate, and thus the Wulff construction can only be rigorously applied if the adhesion energy is included.^{16,17} However, the anisotropy in the surface energy is so extreme that we have also been able to grow pyramidal CCO objects on rocksalt MgO substrates.¹⁸ The objects on this substrate are bigger

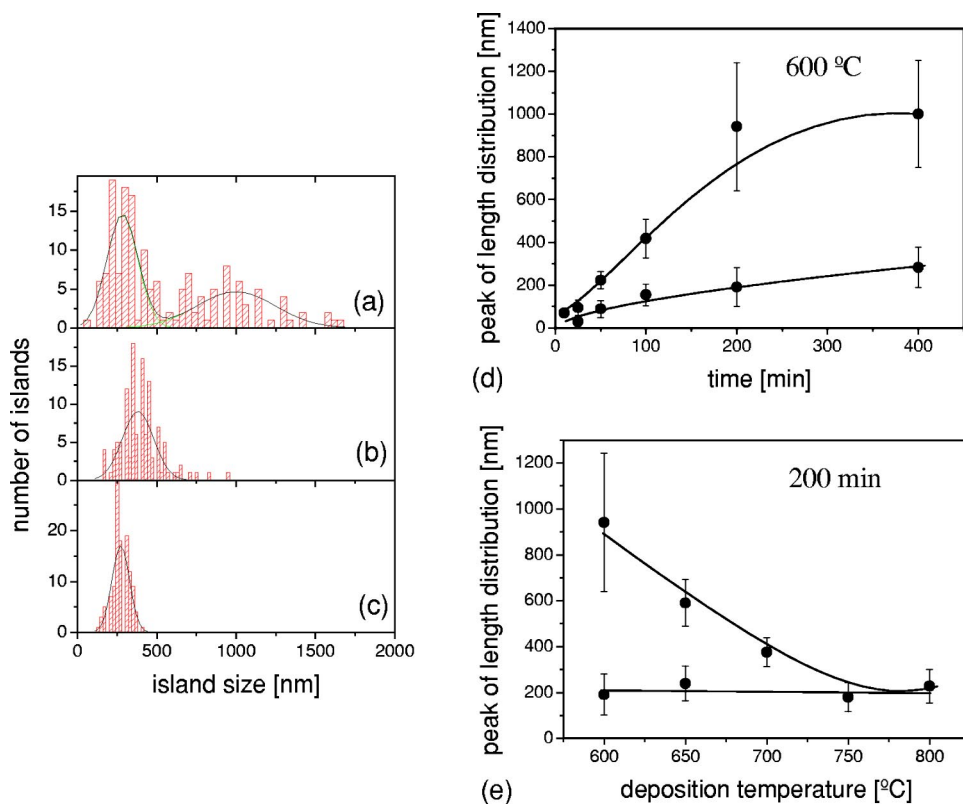


FIG. 3. (Color online) Histograms of (a) the length of islands of the sample prepared at 600°C and 400 min; (b) the length and (c) the width of the sample prepared at 750°C during 200 min. Panels (d) and (e) show the maxima of the length distribution (and their full width at half maximum as error bars) of the islands in films prepared during different sputtering times (d) and substrate temperature (e).

than on MAO for the same deposition time, but the same $\{111\}$ faceted pyramidal shape is observed. In contrast to CCO, in Si the $\{111\}$ planes are of minimum energy,¹⁹ but the difference with the surface energy of the Si(001) plane is only around 10% and does not compensate an increase in the total area. The growth of SiGe pyramids is due to a Stranski-Krastanow mechanism, in which a reduction of the elastic energy is the driving force to overcome the higher area of the surface. Unfortunately, when the SiGe pyramidal objects increase in size the energy relief is more efficient with a higher aspect ratio, which is possible with the introduction of new facets.²⁰ The shape transition from pyramids to domes makes the controlled fabrication of single shaped SiGe dots difficult. In the case of the CCO objects, such a drawback does not exist since minimization of the surface energy is the driving force.

A microscopic explanation of the formation of CCO objects having a narrow size distribution and spatial order, as observed here, is more subtle. The first issue is to establish if the objects are stable against coarsening. We note that when islands are in contact, they remain $\{111\}$ faceted, i.e., no other facets are introduced at the contact zone. This is a consequence of the anisotropy of the surface energy. We also note that the spatial distribution of the family of smaller islands is not affected by the presence of the big islands, i.e., there is not a zone denuded of small islands around the bigger ones. This indicates that small islands, also $\{111\}$ faceted, have to be very stable and hence a migration of their atoms is not expected. In fact, SEM images [Fig. 6(a)] show islands a few tens of nanometers base dimensions which are very close (separations lower than 30 nm are well resolved) to the big ones, i.e., those with hundreds of nanometers of base

dimensions. The stability of the CCO objects was conclusively demonstrated by an additional experiment: a film deposited during 100 min at 600°C was cut in two pieces; one of those was afterwards annealed during 120 min. The SEM images did not reveal appreciable differences between the as-prepared film [Fig. 6(a)] and the annealed one [Fig. 6(b)].

A second issue to be addressed is if the distribution of $\{111\}$ huts and pyramids grows directly on the bare (001)-MAO substrate, i.e., a Volmer-Weber type growth, or if there is an underlying thin layer of (001)-CCO before the growth of $\{111\}$ objects becomes energetically favorable. Considering the hypothesis of an initial growth of an underlying CCO

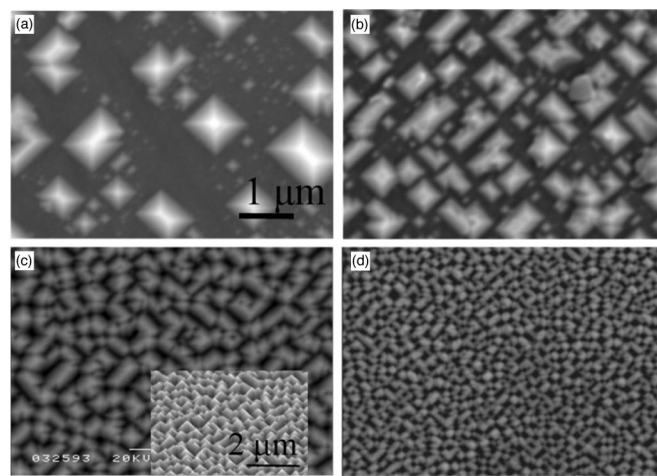


FIG. 4. Scanning electron microscopy images (0° view) of films deposited during 200 min at (a) 600°C; (b) 650°C; (c) 700°C; and (d) 750°C. The inset in (c) is a 45° view.

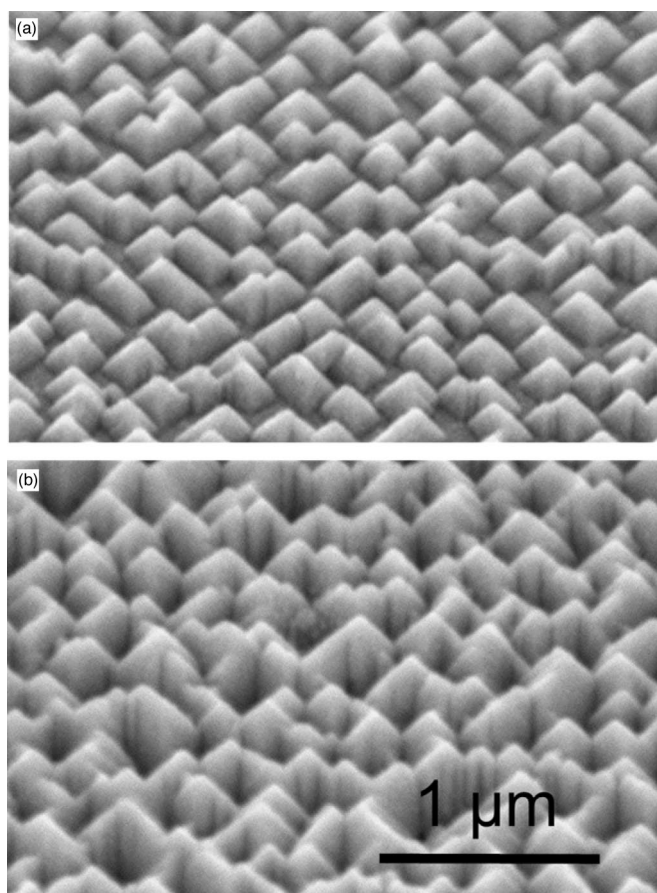


FIG. 5. Scanning electron microscopy images (45° view) of films deposited at 750°C during (a) 100 min and (b) 400 min.

film, we note that in the 50-min sample the islands are much smaller [Fig. 2(a)] than those observed in samples with a higher deposition time, and apparently the total volume of the islands does not scale with deposition time. Therefore, we believe that growth proceeds in two stages: a first one corresponding to the formation of a homogeneous film, and a second one corresponding to the spectacular growth of some islands, whereas the growth rate of the underlying homogeneous film consequently decreases or even vanishes. In order to get insight in to the early stages of growth we prepared thinner films at the low temperature (600°C). The morphology of the film grown during 10 min,¹³ granular-like, is effectively homogeneous and very similar to that of the surface not covered by pyramidal objects in films with longer deposition times. The possibility of a Volmer-Weber growth seems to be unlikely as pyramidal objects should have nucleated directly on the substrate, and therefore should be observable in every stage of growth. However, the structures reported here are well visible only after a thickness around 20 nm.¹³ Further studies of the earlier stages are necessary to discern the growth mechanism of the homogeneous, but granular-like, underlying film.

Next, we should address the question of the origin of the bimodal size distribution. In semiconductors, as previously mentioned, the bimodal distributions are explained as due to phase transitions associated with the shape evolution from pyramids to domes. In contrast, the CCO structures present

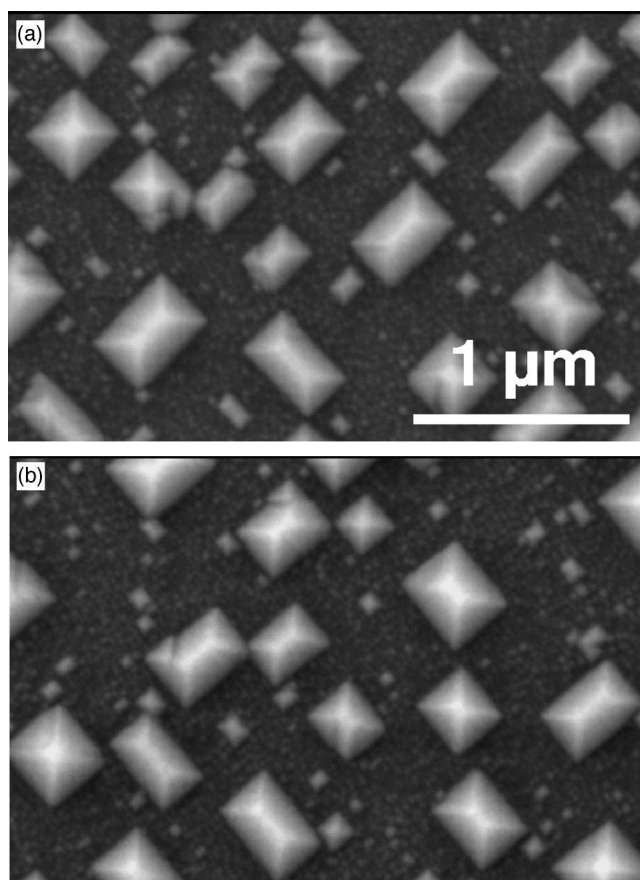


FIG. 6. Scanning electron microscopy images (0° view) of a film deposited during 100 min at 600°C (a) as-prepared, and (b) after being annealed during 120 min at 600°C and 250 mTorr (25% O_2 –75% Ar).

bimodal size distributions despite being $\{111\}$ faceted during all the stages of their growth. We note that the samples are fully relaxed (as deduced from x-ray diffractometry measurements^{12,13}) and we hypothesize that in an early growth stage the plastic (i.e., via dislocations) relaxation of the islands was nonsimultaneous. This assumption implies that for a certain time interval, during the film growth, dislocated and elastically strained islands coexisted. This coexistence may provide a driving force to originate the CCO island size bimodal distribution, as the coexistence could trigger the spectacular growth of a part of the islands, since the chemical potential of the dislocated objects has to be lower than that of the still elastically strained. In fact, a similar scenario was used to account for the spectacular growth of some SiGe domes at high coverage as related to their plastic deformation.^{3,4} We also note that the island size distribution is single-modal and narrower in films prepared at the highest deposition temperatures. This behavior is consistent with the hypothesis of nonsimultaneous initial relaxation, since the energy barriers for the nucleation and propagation of dislocations should be more easily overcome at high temperature. Indeed, the simultaneous island growth that is expected at high temperature explains the smaller size of the structures.

Finally, our films display a long-range ordering of the islands. To understand the cause of this we have to distin-

guish between the orientational and the positional order. The faceted morphology of the islands produces the clear orientational order, since the $\{111\}$ facets intersect the (001) substrate plane in the $\langle 110 \rangle$ directions. The positional order, mostly also along $\langle 110 \rangle$ crystal directions, is defined by the position of the apex of the pyramid or the top edge of the hut clusters, but also by the position of the edges of the bases. This order, not as apparent as the orientational, is emphasized in Fig. 1(b) by inclusion of solid lines to guide the eye. An elastic interaction through the substrate was suggested²¹ to explain the formation of two-dimensional arrays of semiconductor islands. A similar interaction, before CCO relaxation, could be invoked as the driving force to originate the observed long-range positional order. However, this mechanism seems unlikely as the CCO structures are far apart. More work is required to address the origin of the long-range spatial order, with particular attention to the substrate surface.

In summary, a self-organized structure of isolated pyramids and hut clusters with $\{111\}$ facets develops in (001)-oriented epitaxial CCO films. In contrast with semiconductor dots, these objects are true three-dimensional and do not undergo a shape transition. It has been proved that, varying the deposition conditions, the size of the objects can be tuned, and that a $\{111\}$ fully faceted surface can be obtained. We have shown that the anisotropy of the surface energy in spinels is the driving force for the growth of the $\{111\}$ faceted objects, and we have proposed possible mechanisms to

explain the observed size distributions and long-range order. Our findings illustrate that the growth of complex oxides can promote a variety of self-organized morphologies not necessarily predictable from the widely investigated growth of semiconductors and, perhaps, leading to a more reproducible and simpler fabrication process. Even more, the combination of the rich physical properties of complex oxides and the long-range ordering of nano/micro single-faceted objects might lead to other functionalities.

Interestingly enough, since submission of this manuscript, Zheng *et al.*²² have reported the fabrication of arrays of ferrimagnetic CoFe_2O_4 nanopillars—having a spinel structure—embedded in a ferroelectric BaTiO_3 matrix by a self-assembly technique and displaying a remarkable coupling of magnetic and ferroelectric properties not observed in ordinary multilayer structures. To what extent the growth of pyramidal CCO objects reported here could be viewed as a particular stage of growth of the CoFe_2O_4 nanopillars remains to be elucidated.

ACKNOWLEDGMENTS

Financial support by the CICYT of the Spanish Government (Projects MAT2002-04551-C03-01 and MAT2003-4161) is acknowledged. This research has been supported by a Marie Curie Fellowship of the European Community program Human Potential under Contract Number HPMT-CT-2000-00106.

-
- ¹B. Voigtländer, *Surf. Sci. Rep.* **43**, 127 (2001).
²C. Teichert, *Phys. Rep.* **365**, 335 (2002).
³R. S. Williams, G. Medeiros-Ribeiro, T. I. Kamins, and D. A.A. Ohlberg, *Annu. Rev. Phys. Chem.* **51**, 527 (2000).
⁴M. Goryll, L. Vescan, K. Schmidt, S. Mesters, H. Lüth, and K. Szot, *Appl. Phys. Lett.* **71**, 410 (1997).
⁵G. Medeiros-Ribeiro, A. M. Bratkovski, T. I. Kamins, D. A. A. Ohlberg, and R. S. Williams, *Science* **279**, 353 (1998).
⁶T. I. Kamins, E. C. Carr, R. S. Williams, and S. J. Rosner, *J. Appl. Phys.* **81**, 211 (1997).
⁷J. A. Floro, E. Chason, L. B. Freund, R. D. Twisten, R. Q. Hwang, and G. A. Lucadamo, *Phys. Rev. B* **59**, 1990 (1999).
⁸I. Daruka, J. Tersoff, and A.-L. Barabási, *Phys. Rev. Lett.* **82**, 2753 (1999).
⁹R. E. Rudd, G. A. D. Briggs, A. P. Sutton, G. Medeiros-Ribeiro, and R. Stanley Williams, *Phys. Rev. Lett.* **90**, 146101 (2003).
¹⁰Y. Suzuki, R. B. van Dover, E. M. Gyorgy, J. M. Phillips, V. Korenivski, D. J. Werder, C. H. Chen, R. J. Cava, J. J. Krajewski, W. F. Peck, and K. B. Do, *Appl. Phys. Lett.* **68**, 714 (1996).
¹¹G. Hu and Y. Suzuki, *Phys. Rev. Lett.* **89**, 276601 (2002).
¹²U. Lüders, F. Sánchez, and J. Fontcuberta, *Mater. Sci. Eng., B* **109**, 200 (2004).
¹³U. Lüders, F. Sánchez, and J. Fontcuberta, *Appl. Phys. A: Mater. Sci. Process.* **79**, 93 (2004).
¹⁴R. K. Mishra and G. Thomas, *J. Appl. Phys.* **48**, 4576 (1977).
¹⁵R. Dekkers, C. F. Woensdregt, and P. Wollants, *J. Non-Cryst. Solids* **282**, 49 (2001).
¹⁶K. Højrup Hansen, T. Worren, S. Stempel, E. Lægsgaard, M. Bäumer, H. J. Freund, F. Bedenbacher, and I. Stensgaard, *Phys. Rev. Lett.* **83**, 4120 (1999).
¹⁷T. Worren, K. Højrup Hansen, E. Lægsgaard, F. Bedenbacher, and I. Stensgaard, *Surf. Sci.* **477**, 8 (2001).
¹⁸U. Lüders, F. Sánchez, and J. Fontcuberta (unpublished).
¹⁹D. J. Eaglesham, A. E. White, L. C. Feldman, N. Moriya, and D. C. Jacobson, *Phys. Rev. Lett.* **70**, 1643 (1993).
²⁰J. A. Floro, E. Chason, L. B. Freund, R. D. Twisten, R. Q. Hwang, and G. A. Lucadamo, *Phys. Rev. B* **59**, 1990 (1999).
²¹V. A. Shchukin and D. Bimberg, *Rev. Mod. Phys.* **71**, 1125 (1999).
²²H. Zheng, J. Wang, S. E. Lofland, Z. Ma, L. Mohaddes-Ardabili, T. Zhao, L. Salamanca-Riba, S. R. Shinde, S. B. Ogale, F. Bai, D. Viehland, Y. Jia, D. G. Schlom, M. Wuttig, A. Roytburd, and R. Ramesh, *Science* **303**, 601 (2004).